

Fiber Bragg grating sequential UV-writing method with real-time interferometric side-diffraction position monitoring

Kuei-Chu Hsu

Department of Photonics & Institute of Electro-Optical Engineering, National Chiao-Tung University, Hsinchu 300, Taiwan, R.O.C.

Lih-Gen Sheu

Department of Electronic Engineering, Vanung University, Chung-Li, Tao-Yuan 320, Taiwan, R.O.C.

Kai-Ping Chuang

Center for Measurement Standards, Industrial Technology Research Institute, Hsinchu 300, Taiwan, R.O.C.

Shu-Hui Chang and Yinchieh Lai

Department of Photonics & Institute of Electro-Optical Engineering, National Chiao-Tung University, Hsinchu 300, Taiwan, R.O.C.

yclai@mail.nctu.edu.tw

Abstract: This work presents a new sequential UV-writing procedure for fabricating long fiber Bragg grating (FBG) devices. To real-time accurately align the position of every exposed FBG section prior to UV exposure, a single-period reference fiber grating with strong refractive index modulation is probed by applying an interferometric side-diffraction method to measure the grating phase as the position reference. In this way the overlapped FBG sections can be connected section-by-section without obvious phase errors, even when the written index-modulation is weak.

©2005 Optical Society of America

OCIS codes: (120.3180) Interferometry; (230.1480) Bragg reflectors

References and links

1. T. Komukai, K. Tamura, and M. Nakazawa, "An efficient 0.04-nm apodized fiber Bragg grating and its application to narrow-band spectral filtering," *IEEE Photon. Technol. Lett.* **9**, 934-936 (1997).
2. J. T. Kringlebotn, J. L. Archambaut, L. Reekie, and D. N. Payne, "Er³⁺:Yb³⁺-codoped fiber distributed-feedback laser," *Opt. Lett.* **19**, 2101-2103 (1994).
3. Naum K. Berger, Boris Levit, Shimie Atkins, and Baruch Fischer, "Repetition-rate multiplication of optical pulses using uniform fiber Bragg gratings," *Opt. Commun.* **221**, 331-335 (2003).
4. M. J. Cole, W. H. Loh, R. I. Laming, M. N. Zervas and S. Barcelos, "Moving fiber/phase mask-scanning beam technique for enhanced flexibility in producing fibre gratings with uniform phase mask," *Elect. Lett.* **31**, 1488-1490 (1995).
5. I. Petermann, B. Sahlgren, S. Helmfriid, A. T. Friberg, and P.-Y. Fongjallaz, "Fabrication of advanced fiber Bragg gratings by use of sequential writing with a continuous-wave ultraviolet laser source," *Appl. Opt.* **41**, 1051-1056 (2002).
6. F. El-Diasty, A. Heaney, and T. Erdogan, "Analysis of fiber Bragg gratings by a side-diffraction interference technique," *Appl. Opt.* **40**, 890-896 (2001).
7. K.-P. Chuang, I.-L. Wu and Yinchieh Lai, "Interferometric side-diffraction position monitoring technique for writing long fiber Bragg gratings," *CLEO/IQEC, CThM6* (2004).
8. Mattias Åslund, John Canning, Leon Poladian, and C. Martijn de Sterke, "Novel characterization technique with 0.5 ppm spatial accuracy of fringe period in Bragg gratings," *Opt. Express* **11**, 838-842 (2003).
9. K.-P. Chuang, Y. Lai, and L.-G. Sheu, "Pure apodized phase-shifted fiber Bragg gratings fabricated by a two-beam interferometer with polarization control," *IEEE Photon. Technol. Lett.* **16**, 834-836 (2004).
10. B.-O. Guan, H.-Y. Tam, X.-M. Tao, and X.-Y. Dong, "Highly stable fiber Bragg gratings written in hydrogen-loaded fiber," *IEEE Photon. Technol. Lett.* **12**, 1349-1351 (2000).

1. Introduction

Advanced fiber Bragg gratings (FBGs) with complex grating structures of arbitrary phase shifts and refractive index profiles have been continuously attractive for many optical communication applications, including narrow-band FBG DWDM OADMs, dispersion compensators, phase-shifted DFB fiber lasers and pulse repetition-rate multiplication [1-3]. Several procedures that can realize long and complex FBG structures have recently been developed, such as the moving-fiber-scanning-beam technique [4] and the sequential writing techniques [5]. In these methods, a conventional laser interferometer is typically utilized to monitor the fiber/UV-beam position during the writing process. However, accumulative position reading errors due to interferometer drift and inaccurate grating period estimation have caused significant difficulties on the fabrication of long-length fiber Bragg gratings.

To overcome some of these difficulties, in the present paper we utilize the side-diffraction interference method [6] for real-time monitoring the fiber position accurately during the sequential writing process [7]. The side-diffraction interference technique was originally developed for measuring the variation of the grating period and the refractive-index modulation profile of the exposed FBGs [6, 8]. In the literature it has also been suggested that the method can be used as a position control scheme [8]. However, we believe the present paper is the first experimental report on actually using the method for real-time position monitoring during the FBG fabrication process. By directly measuring the grating phase, we can connect adjacent grating sections with accurate phase alignment.

In this work, two real-time side-diffraction position monitoring schemes for fabricating long fiber Bragg gratings are investigated. In the first scheme, the side diffraction position monitoring method that probes the just-exposed grating section has been developed to fabricate single-period fiber Bragg gratings. Because the grating phase of the just-exposed grating section is still affected by the later exposures due to the strongly overlap exposure scheme we use, and because it is difficult to form a clear interference pattern for the side-diffraction measurement when the refractive index modulation is lower than 3.0×10^{-5} , this simple method is only suitable for fabricating single-period fiber FBGs with reasonable strength index modulation. The second scheme employs a reference fiber Bragg grating with a uniform strong refractive index profile fabricated by using the first scheme. The reference grating is placed in parallel to the exposure fiber on the moving stage. Prior to the UV exposure of every FBG section, the reference fiber grating is probed with the side-diffraction method to determine the grating phase as the reference. The measured value can then provide an accurate fiber position reference during the fabrication process. The second scheme shares the same advantage with the first scheme that the accumulative position measurement errors during the long fiber scan can be avoided. Moreover, it also has the following additional advantages. First of all, long FBGs with weak index modulation can be fabricated. The first scheme fails to do this because the resolution of our side-diffraction monitoring scheme is limited to 3.0×10^{-5} refractive index modulation. Secondly, phase shifts along the fiber grating can be easily inserted. The first scheme fails to do this because with the insertion of phase shifts, the grating phase of the just-exposed section will still not reach the final value due to the strongly-overlapped exposure method we use [9]. Thirdly, the required reference FBG can be fabricated by a similar setup (the first scheme) or by different methods (i.e., the phase mask method). In principle, the second scheme will be capable of fabricating arbitrary FBG refractive index modulation profiles with arbitrary grating phase shifts. Details of the experimental setups and the achieved results for the proposed schemes will be presented during the following sections.

2. Real-time side-diffraction position monitoring by probing the just-exposed section

Our first real-time side-diffraction position monitoring method is by probing the just-exposed fiber grating section. Figure 1(a) shows the schematic diagram. A 5-mW single-polarization He-Ne laser beam is expanded with two spherical lenses to achieve a final beam diameter of roughly 3 mm. It is then divided into two probe beams A and B with a polarization beam

splitter. The function of the first half-wave plate is to control the intensity ratio of these two divided beams. The second half-wave plate rotates the polarization of the probe beam B relative to the probe beam A. Probe beam A is then focused onto the exposed fiber with a spherical lens of 20-cm focal length. The first-order Bragg diffraction of probe beam A is generated under the phase-matching Bragg condition $\sin\theta_1 = n_B \cdot \lambda / \lambda_B$, where θ_1 is the input angle of the probe beam in air, n_B is the effective index of the exposed fiber at the Bragg wavelength λ_B , and λ is the wavelength of the probe beam. Probe beam B and diffracted probe beam A are combined at the beam combiner with an interference angle of θ_2 . A 440×480 monochrome CCD camera with a pixel width of 7.15- μm is utilized to record the interference pattern produced by probe beams A and B. The visibility of the interference pattern can be optimized by adjusting the two half-wave plates. A frequency-doubled argon-ion laser launches a CW 244-nm single-polarization ultra-violet (UV) beam into a two-beam interferometer. Exposure of the interference UV beams with the FWHM of 6.5 mm forms a periodic UV intensity pattern onto the exposed fiber to induce a single FBG section. The long fiber Bragg grating is achieved by connecting many strongly-overlapped, equally-spaced, Gaussian-shaped FBG sections with accurate grating phase alignment. A half-wave plate is placed in one path of the two interfering beams to obtain pure apodization (flat DC-index modulation) for the final FBG [9]. The translation stage comprises of a linear motor stage and a piezoelectric translator (PZT) stage with sub-nm position resolution. The accurate alignment of the fiber position is achieved by shifting the translation stage by a given distance and then iteratively fine-tuning the PZT stage according to the grating phase measurement of the just-exposed grating section. In our preliminary experimental setup, the position monitoring accuracy of the whole system is better than 4 nm, but the accuracy of the position-seeking feedback control loop is only set to be around 5 nm (1% of the grating period) in order to reduce the required position-seeking time. The measurement accuracy we have readily achieved is two-fold better than the estimated accuracy in Ref.[8].

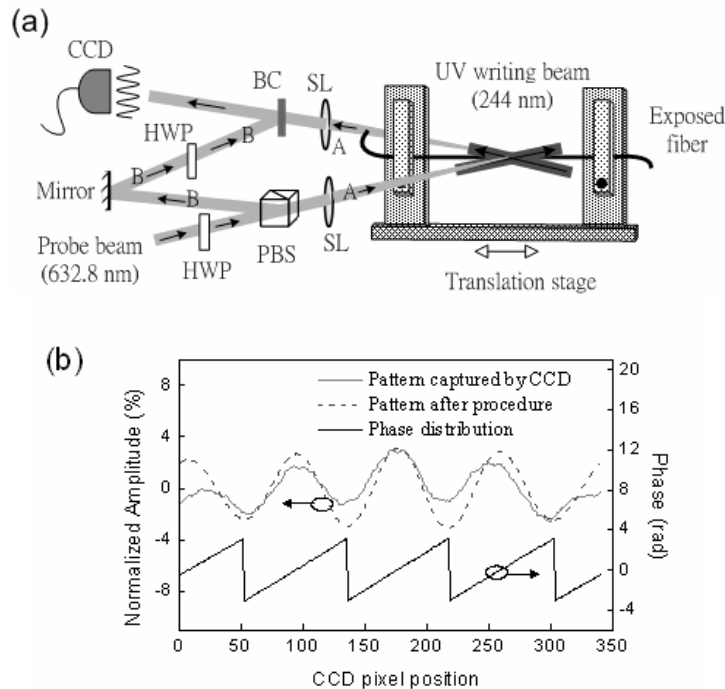


Fig. 1. (a) Real-time side-diffraction position monitoring setup by probing the just-exposed section. SL: spherical lens; BC: beam combiner; PBS: polarization beam splitter; HWP: half wave plate. (b) Typical interference pattern captured by CCD, the pattern after procedure (filtering+taking-real-part) and the calculated phase distribution.

The intensity of the first-order diffracted probe beam A is denoted as I_A , and the intensity of the probe beam B is assumed to be I_B . The intensity distribution of the interference fringe on the CCD along the x-axis, which is perpendicular to the bisector of the two interfering beams, is given by

$$I_{\text{int}} = I_A + I_B + 2\sqrt{I_A I_B} \cdot \cos[kx \cdot 2 \sin(\frac{\theta_2}{2}) + \delta] \quad (1)$$

where $k=2\pi/\lambda$ is the wave vector, θ_2 is the interfering angle and δ is the phase difference between the two interfering beams. The phase difference δ contains two contributions:

$$\delta = \delta_{\text{grating}} + \delta_{\text{path difference}} \quad (2)$$

where δ_{grating} is the phase change of the diffracted probe beam A caused by the fiber grating, and $\delta_{\text{path difference}}$ is the phase change caused by the optical path difference between two probe beams. Since $\delta_{\text{path difference}}$ is constant during the scan, the grating phase change can be inferred from monitoring the phase difference δ . The interference pattern I_{int} is processed by the Fourier transform to obtain the corresponding spatial frequency spectrum. The spectrum is then filtered to keep only the positive frequency part and is inverse-Fourier-transformed back to the original domain. The phase δ can then be identified by taking the arg of the processed data. Figure 1(b) shows the typically resulted periodic pattern captured by the CCD camera (grey solid line), the pattern after the filtering+taking-real-part procedure (grey dotted line) and the obtained phase distribution by taking the arg of the filtered data (bold solid line). For producing single period FBGs, the PZT stage is fine tuned until the just-exposed fiber grating phase distribution obtained in this step is the same as that of last step. The UV-beam shutter is then turned on for writing the present FBG section with a given time duration. In practice, the whole algorithm is implemented with the LabVIEW software for automatically controlling the whole exposure process.

As an example, this side diffraction position monitoring method that probes the just-exposed section has been employed for preparing a single-period fiber grating with strong index-modulation. The fiber used is the photosensitive fiber (Fibercore PS1500) after 1,900-par hydrogen loading at room temperature for several days. The FWHM of the UV beam is about 6.5 mm and the fiber scan step is about 1mm. The final FBG is produced after a 80-section sequential writing to reach a total grating length about 80 mm. The same side-diffraction method [6] is applied to measure the whole refractive index modulation profile of the fabricated fiber grating. Figure 2 shows the measured result. One can see that the fabricated fiber grating profile is substantially uniform. The optical reflection spectrum in the inset of Fig. 2 shows that the Bragg wavelength is 1.546 μm and there should be no obvious phase errors. Such a FBG will be used as the reference grating for the scheme in next section.

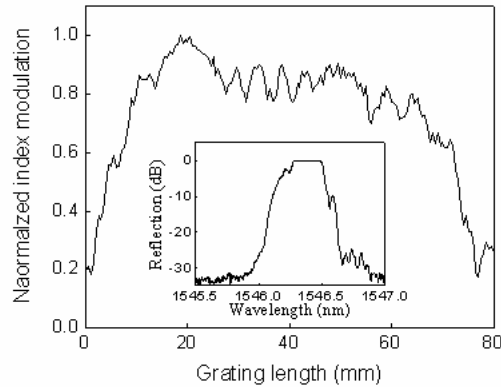


Fig. 2. Refractive index profile and Bragg wavelength of a uniform fiber grating.

3. Real-time side-diffraction position monitoring by probing the reference grating

In the second scheme, the experimental setup includes a reference fiber grating and an exposure fiber which are clamped in parallel on the same moving stage. Figure 3(a) depicts the schematic diagram of the system. The reference grating with a strong and uniform refractive index modulation is prepared in advance with the first scheme. The reference fiber grating under probe is adequately uniform and has a sinusoidal index modulation profile $n(x)$ along its fiber axial direction as

$$n(x) = n_0 + \Delta n \cdot \cos\left(\frac{2\pi x}{\Lambda} + \phi(x)\right) \quad (3)$$

where n_0 is the average refractive index, Δn is the amplitude of refractive index modulation, Λ is the grating period, and $\phi(x)$ describes spatial grating phase. The UV-generated interference period is fine tuned to match the reference fiber grating period, even though this restriction can be relaxed since it will only cause a center-wavelength shift. The accurate alignment of the fiber position is achieved by shifting the translation stage by a given distance and then iteratively fine-tuning the PZT stage according to the reference grating phase measurement. The UV-beam shutter is then turned on for writing the present FBG section with a given time duration. Figure 3(b) reveals the flow chart of the whole operation algorithm. In principle, this method should be able to fabricate long fiber Bragg gratings even when the index-modulation is small and with the option for easy insertion of arbitrary phase shifts.

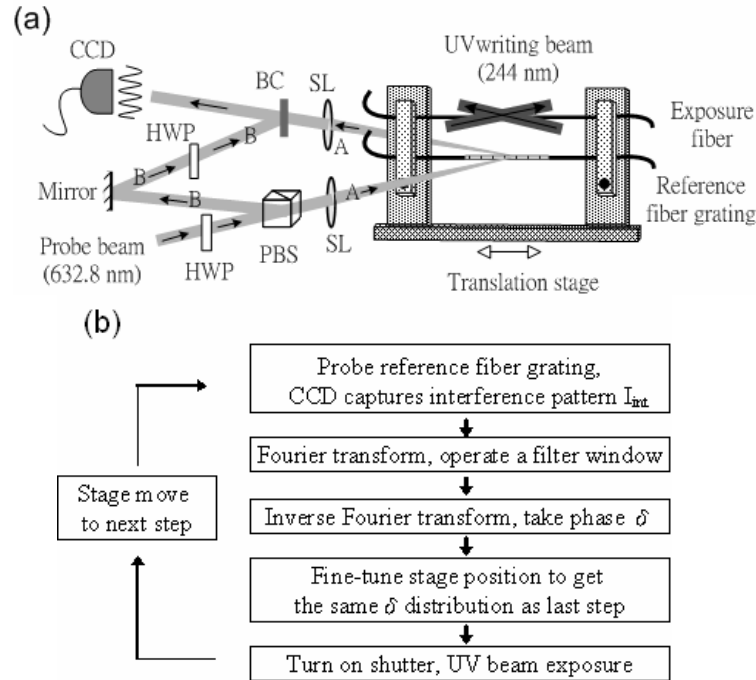


Fig. 3. (a) Real-time side-diffraction position monitoring setup by probing the reference grating. (b) Flow chart of the algorithm.

We have verified the feasibility of the proposed method by two examples. The first example is to fabricate a narrowband, Gaussian apodized FBG with a constant DC refractive index modulation along the whole grating. The reference grating with uniform and strong refractive index modulation is probed to identify the related grating phase information. The FWHM of the UV beam is about 6.5 mm and the fiber scan step is about 1.2 mm. The final FBG is produced after a 58-section sequential writing to reach a total grating length about 70 mm. Before the UV writing process, a DC pre-UV treating process is applied to avoid the nonlinear regime when the exposure UV flux is small [10]. Figure 4(a) shows the reflection and transmission spectra of the exposed FBG. The reflection spectrum has a relatively flat top with the sidelobe level below -20 dB. The 3-dB bandwidth of the reflection spectrum is only 0.07 nm. The peak refractive index modulation is estimated to be 2.5×10^{-5} for this 70-mm-long Gaussian apodized FBG, determined by simulation-fitting. This example demonstrates the feasibility for fabricating long fiber Bragg gratings without noticeable phase errors, even when the written index modulation is below the threshold for reliable side-diffraction measurement.

The second example is to fabricate a 40-mm-long, single π -phase-shifted Gaussian apodized FBG with a constant DC refractive-index modulation. The scan step during the exposure is about 0.6 mm and the final FBG is achieved by connecting 70 FBG sections. A π phase shift is inserted into the center of the exposure fiber grating during the fabrication process. Figure 4(b) shows the reflection and transmission spectrum of the exposure fiber. As expected, there is a narrow transmission peak within the stop-band due to the resonance caused by the π -phase-shift. This simple example demonstrates the feasibility of fabricating phase-shifted FBGs with the new scheme.

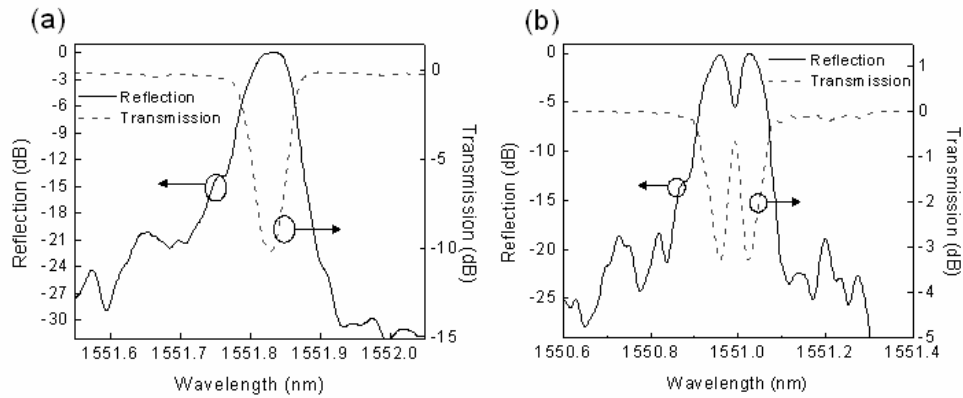


Fig. 4. (a) Reflection and transmission spectra of a 0.07-nm Gaussian apodized 70-mm long FBG. (b) Reflection and transmission spectra of a 40-mm long, π -phase-shift Gaussian apodized FBG.

4. Conclusion

In conclusion, we have proposed and demonstrated a real-time fiber position monitoring method for sequential UV-writing processes by using the interferometric side-diffraction technique. This new method (the second scheme) is capable of fabricating long FBGs with weak index modulation and easily to insert phase shifts along the fiber grating. Furthermore, the required reference FBG can be fabricated by a similar setup (the first scheme) or by different methods (i.e., the phase mask method). Several preliminary examples have been experimentally demonstrated for proving the feasibility of the new method. Hopefully this new method is promising for increasing the accuracy and the ease of fabricating complicated long FBG devices.

Acknowledgments

This research is partially supported by the National Science Council of the Republic of China under the contract NSC 93-2752-E-009-009-PAE and NSC 93-2215-E-009-061. Y. Lai's e-mail address is yclai@mail.nctu.edu.tw.